

Title: Rapid in situ assessment of radiocesium wood contamination using field gamma-ray spectroscopy to optimise felling.

Authors: Adam Varley¹, Andrew Tyler¹, Maksim Kudzin³, Viachaslau Zabrotski³, Justin Brown², Taras Bobrovskyi² and Mark Dowdall².

Affiliations:

¹Department of Biological and Environmental Sciences, University of Stirling, Stirling FK9 4LA, United Kingdom

²Norwegian Radiation Protection Authority, Grini næringspark 13, 1332 Østerås, Norway

³Polessie State Radiation-Ecological Reserve, Tereshkovoy Street 7, Khoyniki, Gomel Region, Belarus

Corresponding author's email address: a.l.varley@stir.ac.uk

Accepted refereed manuscript of:

Varley A, Tyler A, Kudzin M, Zabrotski V, Brown J, Bobrovskyi T & Dowdall M (2020) Rapid in situ assessment of radiocesium wood contamination using field gamma-ray spectroscopy to optimise felling. *Journal of Environmental Radioactivity*, 218, Art. No.: 106259. DOI:

<https://doi.org/10.1016/j.jenvrad.2020.106259>

© 2020, Elsevier. Licensed under the Creative Commons Attribution-NonCommercial-NoDerivatives 4.0 International <http://creativecommons.org/licenses/by-nc-nd/4.0/>

Highlights:

- Characterising caesium contamination in wood is one of the principal issues
- Current methods are inefficient leading to large volumes of waste.
- In situ and mobile gamma-ray spectrometry offer a means of real-time characterisation

Abstract

The Chernobyl nuclear power meltdown that took place in 1986 has left a radioactive contamination legacy that currently severely limits the economic potential of impacted regions including the Polessie State Radioecology Reserve in Southern Belarus. Extensive areas of forested land could potentially become economically viable for firewood and building materials if radioactive contamination, notably ^{137}Cs , could be characterised faster, whilst closely adhering to regulatory limits. Currently, laboursome tree coring and unreliable transfer factors derived from limited soil sampling data are routinely employed in felling decision making, which has financial repercussions owed to the large amounts of waste produced and unnecessary transportation costs. In this study, it is demonstrated that a combination of targeted mobile gamma-ray spectrometry and a newly developed, lead shielded, *in situ* gamma-ray spectrometry method can significantly speed up the process of characterisation of ^{137}Cs wood activity in the field. For the *in situ* method, Monte Carlo calibration routines were developed alongside spectral processing procedures to unfold spectra collected in the field allowing for separation of ground and tree spectral components. Isolated contributions from the tree could then be converted to activity. The method was validated at a test facility and then demonstrated at three separate sites with differing contamination levels. This technique showed that single trees could be measured within approximately 20 % of the activity compared to conventional tree core data. However, some discrepancies were found which were attributed to under sampling using the tree corer and low count rates at the lowest activity site, prompting the need for further data collection to optimise the method. It was concluded that this real-time approach could be a valuable tool for management of contaminated forested areas, releasing valuable timber and ultimately reducing the risk associated with living and working in these areas.

1. Introduction

The Chernobyl accident of April 1986 resulted in the world's largest nuclear disaster, wide scale radioactive contamination being spread over much of Northern Europe with the highest deposition of contamination occurring over large areas of the former USSR countries encompassing modern day Russia, Belarus and Ukraine (IAEA, 2008). Areas in close proximity of the nuclear power plant were particularly impacted leading to evacuation. Large tracts of forested land exist in these regions which are intrinsically linked to efforts towards socio-economic revitalisation of the impacted areas. The most contaminated regions in Belarus occur in the southern reaches of the Gomel Region, along the border with the Ukraine. The Belarusian exclusion zone functions as a scientific reserve, the Polessie State Radiation-Ecological Reserve (PSRER), which covers some 216 thousand hectares. The PSRER is located in a subzone of foliar (deciduous and broad-leaved) and pine woods, with forested areas constituting 109.7 thousand hectares (51.1 % of the territory). Pine woods comprise 43.9 % of the afforested areas, birch woods 30.7 %, black alder 12.4 %, oak 6.3 % and other species 6.7 %. The territories not covered by forest (primarily abandoned agricultural lands) are 82.2 thousand hectares (38.0 %) and non-agricultural unforested lands occupy 20.1 thousand hectares (9.3 %) (Izrael et al., 1996).

Until recent years, the management of Chernobyl contaminated land, inclusive of the PSRER, has been primarily oriented towards reducing external and internal doses to the public and mitigating the risks for further dispersal of contaminants through natural events such as forestfires or wildfires (Dvornik et al., 2018; Evangeliou, 2015). Irrespective of the radiological challenges posed by contamination for forestry workers or residents of forested areas, there are still direct and indirect economic impacts imposed due to radioactive contamination of forests (Yoshihara et al., 2014). This is primarily in relation to regulatory limits imposed on wood and wood products and their effects on the development of forestry resources (Shaw et al., 2001). The important role of forestry and derived products in the current and future Belarusian economy is well established (Gerasimov and Karjalainen, 2010). The area of Belarus with the most forest coverage is the Gomel region and some 2 million ha (21 % of the forest fund area) continues to be impacted by contamination derived from Chernobyl (Woodfuels Program, 2009). Wood harvesting is prohibited in areas with contamination densities in excess of 1.4 MBq m⁻². Relevant regulatory limits for Belarus are displayed in Table 1.

34 Table 1. National admissible levels for the ^{137}Cs content of timber, timber goods and other
 35 non-food forestry products in Belarus (RDU/LH-2001, 2001)

Product/Material	^{137}Cs , Bq/kg
Roundwood for construction of the walls of residential housing	740
Other roundwood products	1480
Process wood	1480
Fuel wood	740
Lumber, wooden goods and construction components (internal) for residential housing	740
Lumber, wooden goods and components, other	1850
Other inedible products	1850

37 Until recently, the assessment of ^{137}Cs content in contaminated forest stands has largely been
 38 based on transfer factors (TF; $\text{Bq kg}^{-1}/\text{Bq m}^{-2}$) that are based on comparing the ^{137}Cs
 39 concentration in a given tree component (Bq kg^{-1}) to the total ^{137}Cs contamination density of
 40 the soil (Bq m^{-2}) (Nimis, 1996). Many TF models have been developed using various different
 41 radionuclide, tree and soil types and have been widely used to assess the redistribution of ^{137}Cs
 42 in forest ecosystems (Ipatyev et al., 1999) and to develop broad-scale maps of forest
 43 contamination from ^{137}Cs deposition inventories (Goor and Avila, 2003; van der Perk et al.,
 44 2004). In terms of building up a general picture of wood activity across a region, TF are a
 45 practical solution given that they can be derived within a relatively short time frame either
 46 through direct soil sampling or using pre-existing decay-corrected soil activity data, combined
 47 with soil composition and land cover maps. However, predictions on a smaller scale, which
 48 are more relevant to the forestry industry, such as over tens of meters, are far more difficult
 49 owing to the environment being innately heterogeneous in terms of soil, tree type and
 50 contamination distribution. Small scale variation in contamination distribution is particularly
 51 important, as more recent studies have demonstrated that orders of magnitude of change can
 52 be observed in areas closer to the Chernobyl nuclear power plant (Golosov, 2003; Golosov et
 53 al., 2000; Adam Varley et al., 2017; Vitaly et al., 2019, 2018). In part this variation is due to

remobilisation, but mainly it is down to finer scale deposition patterns dictated by localised meteorological events in 1986 (Varley et al., 2018). Therefore, basing wood activities for an entire forest stand from TR derived from limited soil samples leaves a study particularly vulnerable to very large uncertainties on final estimates.

The social and economic role of forestry and its products and potential future commercial development of contaminated forestry areas necessitates a means of reliably and efficiently assessing the ^{137}Cs content of trees. Sampling of trees by coring followed by laboratory analysis is inefficient due to the number of trees involved and the time and resources required for sampling and analysis prior to felling. Similarly, alternative methods based on TF's operated over large areas can be unreliable potentially misclassifying large areas of otherwise productive forest stand whilst still requiring analysis of potentially unrepresentative soil samples.

The ability to reliably estimate the ^{137}Cs level in the wood of a tree, in real-time, without the need to fell a tree provides a potentially valuable tool for the forestry industry in areas that are affected by radioactive contamination. Such a tool would significantly reduce waste as trees can be screened prior to felling to ensure compliance with regulatory limits and harvesting effort and resources can be more efficiently applied. In this context, the in situ measurement of ^{137}Cs in standing trees may offer potential benefits.

1.1. Field gamma-ray spectrometry of ^{137}Cs

Conventionally, in situ measurements serve to establish the ^{137}Cs activity deposition (Bq m^{-2}) in the underlying soil and utilise the number of counts in the photopeak at 662 keV (Tyler, 2008). Signal contributions from other environmental media, for example trees, are typically assumed to be negligible or constant, although attempts have been made at characterising contributions from tree trunks and the canopy (Cresswell et al., 2016; Gering et al., 2002). For measurements of the soil activity, a single measurement can be made to derive spatially integrated activity estimates with appropriate correction, from soil core data or estimated from inherent spectral features such as the peak-to-valley ratio (Östlund et al., 2015), for vertical depth distribution of ^{137}Cs (Miller et al., 1990).

However, the use of in situ gamma spectrometry cannot be applied in determining the activity present in a tree by simply placing a detector against the tree as there are almost always two significant signal components: (i) from the contaminants in the tree; and (ii) from the

contaminants in ground. Untangling the signal is unfeasible as contributions from both (i) and (ii) can change significantly on both spatial and temporal scales depending on the amount of ^{137}Cs originally deposited, the properties of the soil and the age and species of the tree (Fogh and Andersson, 2001). In addition, the primary component of the gamma photon signal in the detector would be nuisance signal from the ground as the volume of soil within the field of view of the detector is much larger compared to volume of the tree within the same field of view (Gering et al., 2002). Furthermore, activities in the ground are orders of magnitude higher due to low uptake by the tree from the ground.

The next step is to take two or more separate measurements and try to separate the individual components of the signal using mathematical techniques. This study explores an approach employing strategically placed lead shielding around and in front of the detector to collimate the signal from the tree, thus reducing background signal and canopy signal and ultimately increasing the signal to noise ratio. Crucially, this setup ensures the detector remains in a constant position, negating any issues associated with changes in background and wood heterogeneity. In the past, a similar technique has been adopted with in situ gamma-ray spectrometry, wherein lead shielding was used to collimate the detector's field of view to assess the ^{137}Cs depth distribution (Benke and Kearfott, 2002). The depth of burial was also estimated by using a faceplate to change the angular response of the detector to the source (Feng et al., 2012).

The aim of this study was to develop a system that can quickly estimate the ^{137}Cs concentration within the wood of the tree for a more efficient means of identifying trees that could be felled for economic exploitation and reduce the need for intrusive sampling. The approach utilises Monte Carlo simulations to model the gamma photon spectra to identify the optimal geometries and shielding requirements for differing thicknesses of the tree and distribution of ^{137}Cs throughout a tree trunk. Calibration factors were derived from simulations alongside the development of regular algebraic solutions to allow careful separation of ground and tree contributions. The approach to estimate ^{137}Cs activity is validated from samples taken of trees measured using the shielded detector.

2. Methods

2.1. Measurement procedure and spectral processing

The first step in the measurement process involves measuring the circumference of the tree to be used in the calculation of calibration coefficients to account for its diameter (Graphical abstract - A). The sodium iodide detector is then fastened to the tree trunk at a height of a 1 m and the first measurement is taken with the lead shield open (without the front face plug), exposing the tree to the detector, the face of which is positioned 2 cm back from the front of the lead collimator (Figure 1).

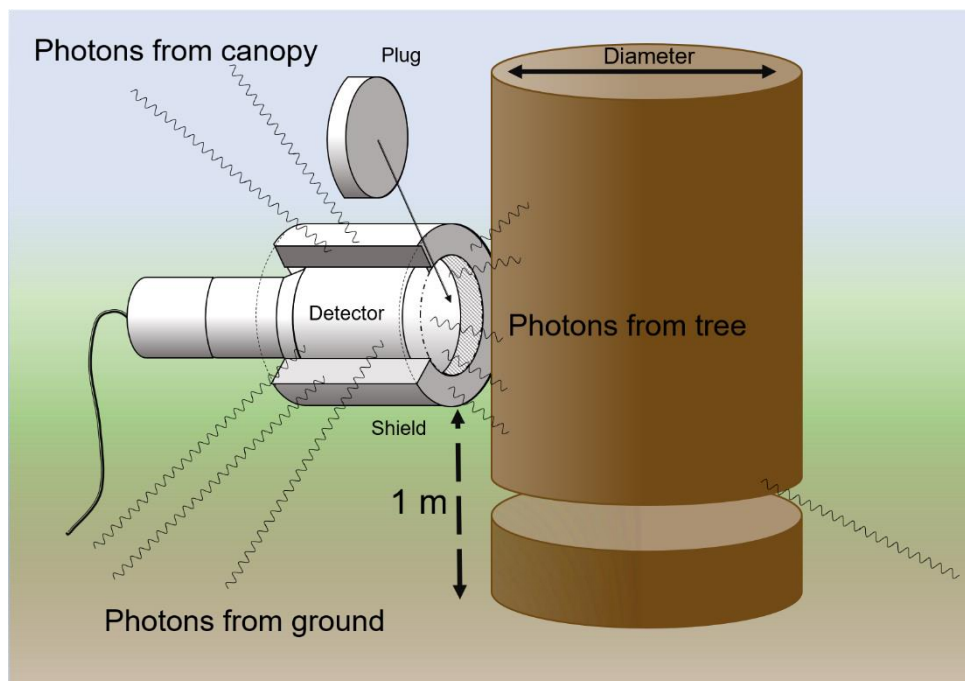
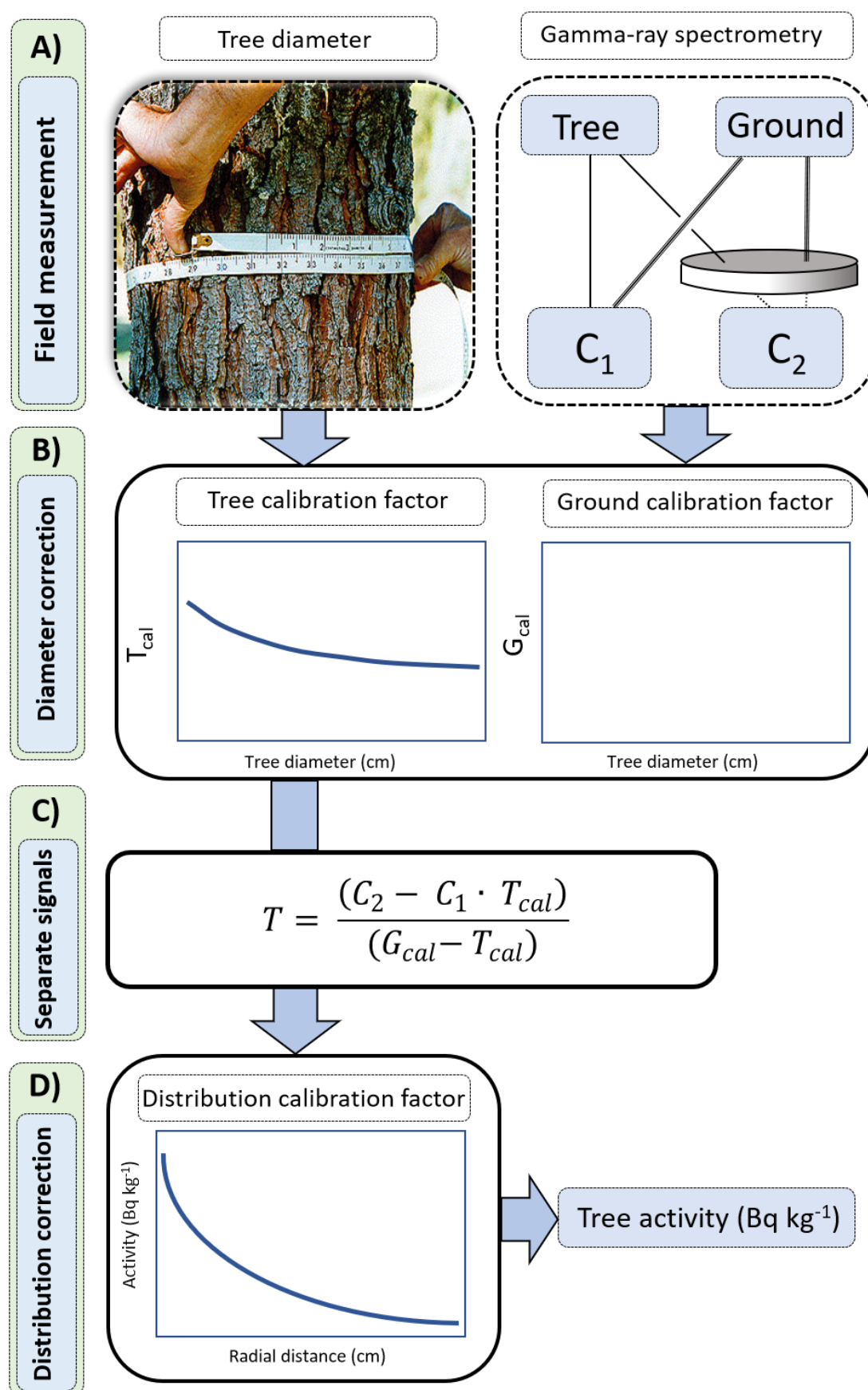


Figure 1. Schematic drawing of the detector, lead collimator and plug.

This measurement produces the count rate C_1 ; referred to as the unshielded measurement, which is made up of counts derived from the ground (G) and Tree (T) (Eq. 1). The second measurement is made when the plug is placed in the collimator and aims to eliminate as much of the tree signal as possible and the resultant signal can be considered as a background (Figure 2A). Nevertheless, significant contributions from both ground and tree will still be observed in the count rate (C_2) that need to be characterised using separate ground and tree calibration coefficients, G_{cal} and T_{cal} , respectively (Eq. 2).



129

130 Figure 2. Flow diagram describing the in situ measurement of ^{137}Cs

131

$$C_1 = G + T \quad (1)$$

132

$$C_2 = G \cdot G_{cal} + T \cdot T_{cal} \quad (2)$$

133 Derivation of calibration coefficients is performed in the second step and account for the
 134 shielding effect of the tree and plug (Figure 2B). The shielding effect from the plug is relatively
 135 constant yet changes in tree diameter will have two effects on the number of photons in both
 136 C_1 and C_2 (eq. 1 and 2). Photons coming from the tree will generally increase with increasing
 137 tree diameter, given that there is more source volume contributing photons although the source
 138 distance will be larger for photons from the edges of the tree. At the same time, counts coming
 139 from the ground will generally decrease with increasing thickness as the tree will be providing
 140 more shielding for photons coming from behind the tree. Acting in combination, these two
 141 effects are likely to have a nonlinear relationship with tree diameter. Consequently, the
 142 relationship between the ratio of shielded and unshielded counts must be characterised in
 143 sufficient detail across a range of diameters forming two calibration coefficients G_{cal} and T_{cal}
 144 where G_{cal} is the ratio between unshielded (G_U) and shielded (G_S) ground counts, and T_{cal} is the
 145 ratio between unshielded (T_U) and shielded (T_S) tree counts described in equation's 3 and 4,
 146 respectively. Essentially, each calibration coefficient is a fraction of the unshielded count.

147

$$G_{cal} = \frac{G_U}{G_S} \quad (3)$$

148

$$T_{cal} = \frac{T_U}{T_S} \quad (4)$$

149 In the third stage, equations (1) and (2) can be combined and rearranged allowing for separation
 150 of the tree signal (T) (eq. 5) (Figure 2C). T represents the number of counts received by the
 151 detector, originating from the tree in the unshielded measurement and can be converted into
 152 activity using Monte Carlo simulations.

153

$$T = \frac{(C_2 - C_1 \cdot T_{cal})}{(G_{cal} - T_{cal})} \quad (5)$$

Prior to this crucial step, a correction factor must be applied to T to account for the radial distribution in the tree (Figure 2D). The observed radial distribution within a tree is due to a number of factors including deposition rates and soil type (Soukhova et al., 2003), although the primary driving force is believed to be due to the biological mobility of radiocaesium within wood, which is dependent on the species and age of the tree. In general, accumulation of caesium tends to occur in the bark and newer growth close to the phloem through which nutrients are transported to the roots. Contrastingly, lower concentrations are found in the pith and older wood towards the centre where water is transferred up to the crown and into the leaves. Importantly, differences in radial distribution can significantly influence the count rate received by the detector and considerable caution must be applied during the application of any correction factors.

$$A = P + (A_0 - P)e^{-cd} \quad (6)$$

From information gained from field observations, and literature values, a simplified model described by an exponential function was used to model caesium radial distribution to correct count rate to activity (Eq. 6). Activity (A) was predicted at radial depth (d) reducing according to the decay constant (c), where A_0 is the activity of the outer layer of bark and P is the activity in the pith. A visual example of a radial distribution is provided in Figure 2 in the supplementary materials using values of 1.5 and 0.1 for c and P , respectively. Although this distribution would suggest that contributions from the bark would have a significant effect on the count rate, it has been calculated that less than 4 % of the counts originate from the bark for this distribution. For larger diameters it is significantly less than 4 %. Importantly, even though the bark is closer to the detector, its relatively small mass contributes relatively little to the overall count rate compared to the rest of the tree.

2.2. Monte Carlo simulations

Calibration of the detector was performed using Monte Carlo simulations, which allowed for complex parameters such as tree diameter and radial distribution to be changed that would otherwise be unfeasible to do so through traditional analytical calibration procedures. A

detailed description of the modelling stage, including geometry specifications and processing routines can be found in the supplementary materials.

2.3. Field sites and measurement

To test the approach, three field sites were selected within the PSRER in the Gomel region of Belarus. The areas were specifically chosen as they covered a broad range of caesium depositions. The chosen three locations were Tulgovichskoe (low activity), Vorotetskoe (medium activity) and Krukovskoe (high activity). Locations of the three sites relative to the Chernobyl NPP are shown in Figure 3 with further details provided in Table 2 supplementary materials; based on five soil samples and corresponding dose rate measurements at each site.

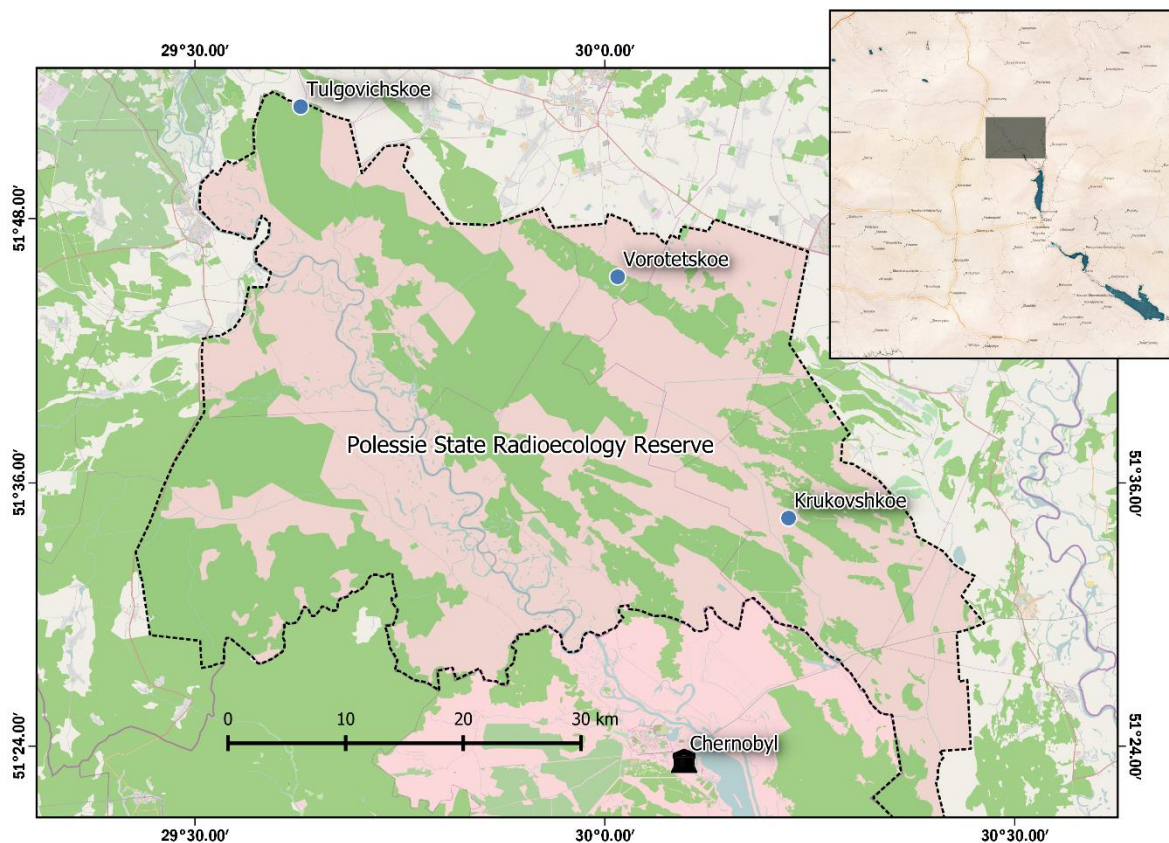


Figure 3. Three test sites relative to the Chernobyl NPP. The dashed line indicates the boundary of the Polessie Radiation Ecology Reserve.

The Tulgovichskoe site was being actively logged as the stands at the site were deemed to be under the relevant regulatory limits (Table 1), whereas the Vorotetskoe and Krukovskoe sites had been untouched since 1986 as they were considered near to or over Belarussian statutory limits with respect to ^{137}Cs content (740 Bq kg^{-1}). A rectangular area (approximately $30 \times 30 \text{ m}$) in which the dose rate was deemed to be the most stable spatially was identified at each of the three forestry sites. The spatial distribution of ^{137}Cs was mapped at each site using a $76 \times 76 \text{ mm NaI:Tl}$ detector integrated with a high accuracy DGPS which provided reliable accuracy under trees for 30 minutes once a signal had been attained. Individual spectra were converted to ^{137}Cs inventory by following the procedure outlined in Varley et al. (2017).

Within the selected mapped areas, 10 mature trees were randomly chosen to test the in situ method and a subset of 4 trees was randomly selected for wood and bark sampling prior to the in situ gamma-ray measurement. Trees were randomly selected by randomly generating coordinates in the map and selecting the closest tree to that coordinate. Wood samples were taken with a tree corer (Haglöf, 5.15 mm diameter, length 300 mm). The remaining 6 trees were not physically sampled, but in situ measurements were performed. Three trees from the Vorotetskoe and Krukovskoe sites were felled to serve as test logs: one pine (*Pinus sylvestris*) from Vorotetskoe, one pine from Krukovskoe and one birch (*Betula pendula*) from Vorotetskoe. The felled trees were moved to an unforested area of low ^{137}Cs activity ($\sim 333 \text{ Bq kg}^{-1}$) producing negligible counts from the background. This area was referred to as the test facility. Samples were taken from test logs from the duramen (dead, central heartwood) and the alburnum (the living secondary sapwood) using a chainsaw alongside bark samples taken with an axe. Samples of each of these three materials were then analysed by HPGe in the laboratory for ^{137}Cs content.

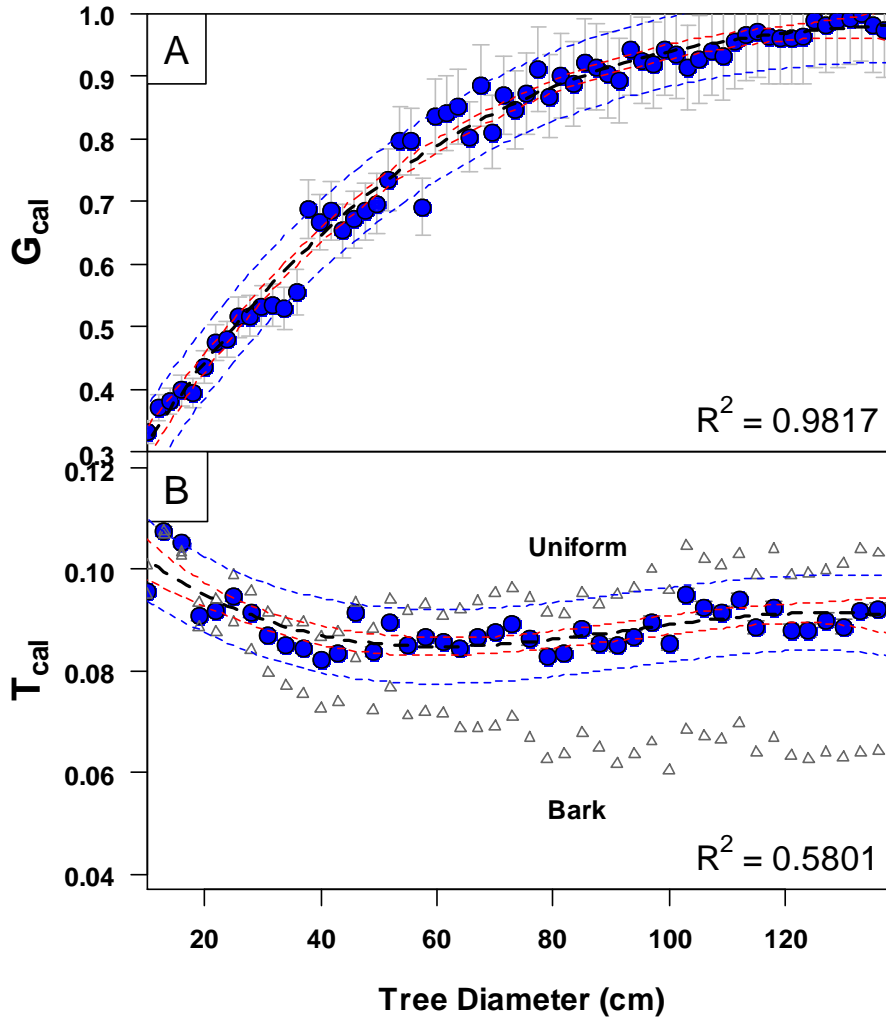
In situ measurements were taken with an InspectorTM 1000 from Canberra and count times were of the order of 3 – 5 minutes, typically resulting in a counting uncertainty under the full energy peak at 661 keV of below 2%.

3. Results and Discussion

3.1. Monte Carlo results

Tree and ground results derived from Monte Carlo give insight into how the detection system interacts with the shield, plug, ground and tree (Figure 4). For the ground model changes in tree diameter effectively introduce shielding and this can be realised as a gradual decrease in the number of counts entering through the front face of the detector in the unshielded (G_U) measurement. Concurrently, this has less of an effect on the shielded measurement (G_S) as it is already partially shielded by the plug. Acting in combination to produce the value G_{cal} , the ratio between G_U and G_S effectively enters a state of equilibrium ($G_{cal} = 1$) at around 120 cm, as this thickness of the tree effectively shields all photon coming from the front face (Figure 4A). Across a typical tree diameter range, G_{cal} can vary by up to 70 %. Importantly, it is this relationship that allows the method to work and for the signal to be separated. The diameter of the tree can be inputted into the model and for a certain diameter of tree, the drop in count rate can be predicted from G_{cal} leaving the tree count rate.

It is a different case for T_{cal} , where the influence of the tree diameter has very little effect on the ratio between unshielded (T_U) and shielded (T_S) measurements, where only minor variations in T_{cal} are witnessed (8 - 10 %) across the diameter range (Figure 4B). Notice that the radial distribution can have a slight influence on T_{cal} , for example the difference between a uniform and a distribution mostly associated with the bark. Yet, in terms of potential uncertainty, this is low in comparison to the final calibration stage in Eq 6, where large variations in radial depth distribution could introduce orders of magnitude of change in the count rate for the same overall activity.



243

244 Figure 4. Model fits derived from Monte Carlo data for ground (A) and tree (B) calibration
 245 factors, G_{cal} and T_{cal} , as a function of tree diameter. Fitted polynomial models display both
 246 confidence (red broken lines) and prediction (blue lines) intervals at 95% and error bars
 247 represent counting uncertainty (1σ). Triangles show the influence of tree diamtere on T_{cal} when
 248 ^{137}Cs is either distributed uniformly throughout the trunk or located predominantly in the bark.

249 3.2. Test logs

250 To test the performance of the detector and shield within a relatively controlled environment,
 251 measurements were taken from three test logs (taken from high activity areas) over relatively
 252 low activity ground. In this scenario, the count rate from the log was many orders of magnitude
 253 higher than the background. These controlled conditions allowed Monte Carlo results derived
 254 purely for the tree to be assessed without significant contribution from the ground and
 255 importantly provide verification for the distribution model.

Observing the ratio between duramen (heartwood) and alburnum (sapwood) ^{137}Cs concentrations in wood tissue between the pine logs and birch logs confirmed that the trees have different radial distributions, but still contain higher contamination towards the outside of the tree in the living wood and the bark (Table 4 in supplementary material). By analysing the duramen/alburnum ratio it becomes clear that contamination within pine species (0.442-0.482) tends to be closer to the bark of the tree compared to the birch tree (1.080-1.230) (Table 2). This finding matches general patterns found by other studies on distributions of this isotope in trees (Ohashi et al., 2014; Soukhova et al., 2003). The limited sample size was not enough to draw significant conclusion on radial distribution but was enough to approximately parameterise Monte Carlo models to derive activity estimates from in situ count rates.

Table 2. Cs-137 activity concentrations in various radial sections of the test logs based on laboratory measurement. Measurement uncertainties 2σ for laboratory and *in situ* measurements.

Test log	Average wood activity (Bq kg^{-1})	In situ estimate (Bq kg^{-1})	Duramen/alburnum activity concentration ratio
Pine (Krukovskoe) – base of log	4220 ± 1200	4260 ± 1350	0.442
Pine (Krukovskoe) – top of log	5170 ± 1460	5200 ± 1800	0.456
Pine (Vorotetskoe) – base of log	841 ± 249	816 ± 315	0.482
Pine (Vorotetskoe) – top of log	619 ± 182	664 ± 249	0.454
Birch (Vorotetskoe) – base of log	551 ± 157	716 ± 283	1.080
Birch(Vorotetskoe) – top of log	452 ± 131	507 ± 205	1.230

Laboratory results from wood samples taken from the test facility were compared to measurements made along the logs using the in situ detector (Table 2). In situ measurements were calibrated using the conservative parameters from the radial distribution data for the pine test logs. It was decided that due to the potentially more complex distribution within the birch trees, and the smaller amount of data available, the pine distribution would be fitted to the birch tree results. Furthermore, the pine distribution was more relevant to this study as most of the trees that were measured in the field were Scots Pine trees.

Wood samples and in situ activity estimates were within 7 % of each other for the test pine logs. Wood activity estimates for the birch log were less reliable ($< 25\%$), this is understandable given that the exponential radial distribution that was fitted to the pine data will be different compared to that of a typical birch radial distribution (Table 2).

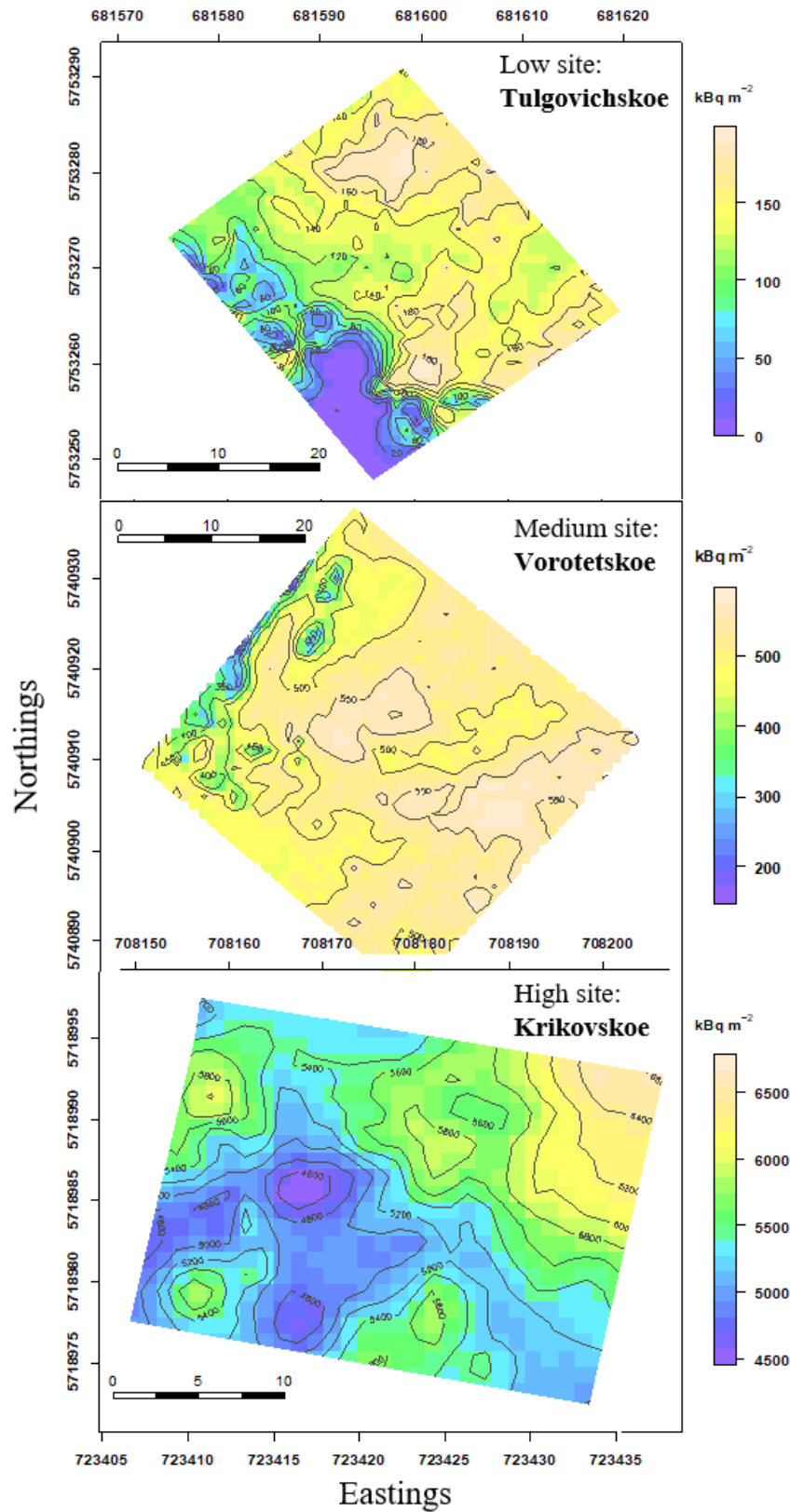
3.3. *Soil transfer factors*

As discussed earlier, the conventional way of estimating activity levels in trees is by use of concentration ratios. A statistical summary of ^{137}Cs concentration ratios for various groups of relevance to this study is shown in Table S2 in the supplementary materials which was extracted from IAEA (2014).

The most suitable values to apply were from the category ‘Trees: broad-leaf’ for birch and ‘Trees coniferous’ for pine, albeit that essentially identical concentration ratios are provided for both categories. The underlying datasets used to derive transfer factors are generally considered to be characterised by log-normal distributions (Sheppard, 2005) and thus the geometric mean provides the most appropriate selection for a best estimate or central tendency of the CR value (see Table S3 in the supplementary materials).

3.4. *Field site deposition patterns*

Although site selection aimed to find 3 areas that were relatively spatially uniform, mapped by mobile gamma-ray spectroscopy results, indicate that there was considerable heterogeneity across all 3 sites Figure 5 . This is not a surprising result given that across much of the exclusion zone contamination tends to be heterogeneous and can be difficult to characterise without equipment such as a mobile gamma-ray spectrometry operating a spatially sensitive differential GPS. Although not displayed, little difference in ^{137}Cs depth distribution, derived using the peak-to-valley ratio, was found within each site. Between sites there was also not a significant difference in depth. Most of the contamination was estimated to be within the top 10 cm of the soil surface



301

302 Figure 5. Spatial distribution of ^{137}Cs at each of the three sites chosen for the study.

The capability to map contamination at high spatial resolution raises potential issues in using transfer factor approaches that rely on a small amount of soil samples to statistically derive soil activity. At each of the three sites, clearly issues could be encountered using a limited soil sampling size within a heterogeneous environment. In this scenario, the true value of mobile gamma-ray spectrometry becomes clear, as these measurements by themselves could quite easily be used to inform transfer factors and provide a rapid means of characterising forest stands. After which measurements could be used to target the *in situ* method on specific trees.

3.5. Wood activity estimates

In general, good agreement is seen between *in situ* wood activity estimates (Bq kg^{-1}) and wood activities taken using coring device (Table 3). In particular ID 1-5, taken at the high activity site (Krukovskoe) shows a deviation of less than 20 % with exception of ID 3 (~50 % deviation). This high level of agreement could be attributed to the diameter of the trees being relatively small and being relatively consistent across the site. Not only did this make *in situ* measurements easier and the modelling process more straightforward, but the corer could reach closer to the centre of the tree providing a representative sample of wood throughout the radial distribution and would result in more consistency between trees. Furthermore, a low counting uncertainty could be achieved in a relatively short amount of time due to the high levels of contamination.

Trees that were measured using the *in situ* detector, but did not have corresponding wood sample data, still adhered closely to wood activity estimates from nearby trees for which wood sample data was available suggesting that wood activity was reasonably consistent across the site (3200-5330 Bq kg^{-1}). The variability present at this site is, interestingly, comparable to the variability shown across the site from that identified using mobile gamma-ray spectrometry (Table 5 in the supplementary materials). GPS coordinates taken in the field to mark trees were accrued using a standard GPS without differential correction and were not reliable enough to allow for direct comparison.

Activities estimated from the medium activity site (Vorotetskoe) were for the most part reflective of wood sampling estimates (~20 %) for IDs 12-14. *In situ* estimates for ID 15 were considerably different to the wood estimate (>55 %). This disparity could be caused by the trees especially large diameter meaning that the 300 mm coring device probably significantly under sampled the middle of the tree taking relatively more of the higher activity wood present in the

sapwood. Examination of the rest of the in situ measurements without matching wood sample data tends to support this argument as many of the predicted wood activities were between 382-529 Bq kg⁻¹ (Table 3).

The least comparable results were found at the lowest activity site. Notice that the in situ estimate (125 ± 44 Bq kg⁻¹) for ID 21 is over 2 times that of the wood estimate (54 ± 12 Bq kg⁻¹). However, these results were proved not to be significantly different using a one-way ANOVA. Interestingly this was the only birch tree measured in the field and, in concurrence with the test logs, an overestimate of activity was found. This is most likely a consequence of the model being inappropriate for the birch tree radial distribution as it was fitted to pine tree data. However, further deviations of 100 % were found for the remaining two pine trees, although these were not found to be significantly different. These results are harder to explain as the wood sample estimates are lower than the in situ estimates, which cannot be explained by the larger diameters of the trees such as the case at the medium site. Ascertaining the exact reason for this outcome is difficult, although perhaps the low count rates at this site played a significant role and increased uncertainty. Another possibility is that the radial distribution could have been considerably different at this site as is the forest stand was visually very different and contained a greater diversity of trees and had a different soil type. It is evident that further research is required to resolve this issue.

Estimates made using the TR method were fairly robust in terms of encapsulating the maximum and minimum bounds of the wood sampled activity estimates and the in situ and mobile gamma-ray spectrometry activity estimates. It is understandable why TR are widely adopted particularly if there are only soil activity estimates available.

362

363

364

365

Table 3. Wood activity at field sites derived from wood cores, in situ measurements and transfer factors. Measurement uncertainties are quoted to 2σ .

Site	ID	Tree circumference (cm)	Species	Core samples	In situ	Transfer factor
				Wood activity (Bq kg ⁻¹)	Wood activity (Bq kg ⁻¹)	Wood activity (Bq kg ⁻¹)
Krukovskoe	1	141	Pine	3410 ± 705	3310 ± 1050	2040 – 6350
Krukovskoe	2	122	Pine	3200 ± 680	3930 ± 1270	2040 – 6350
Krukovskoe	3	122	Pine	3200 ± 680	4900 ± 1610	2040 – 6350
Krukovskoe	4	96	Pine	4010 ± 840	4490 ± 1550	2040 – 6350
Krukovskoe	5	82	Pine	3600 ± 750	4280 ± 1452	2040 – 6350
Krukovskoe	6	117	Pine	-	4160 ± 1400	2040 – 6350
Krukovskoe	7	118	Pine	-	3270 ± 1200	2040 – 6350
Krukovskoe	8	138	Pine	-	3200 ± 1010	2040 – 6350
Krukovskoe	9	119	Pine	-	4110 ± 1370	2040 – 6350
Krukovskoe	10	87	Pine	-	5330 ± 2010	2040 – 6350
Krukovskoe	11	120	Pine	-	3670 ± 1220	2040 – 6350
Vorotetskoe	12	114	Pine	578 ± 123	521 ± 177	260 - 545
Vorotetskoe	13	169	Pine	575 ± 125	463 ± 162	260 - 545
Vorotetskoe	14	169	Pine	575 ± 125	445 ± 156	260 - 545
Vorotetskoe	15	178	Pine	1010 ± 209	435 ± 158	260 - 545
Vorotetskoe	16	114	Pine	-	593 ± 201	260 - 545
Vorotetskoe	17	111	Pine	-	417 ± 143	260 - 545
Vorotetskoe	18	112	Pine	-	382 ± 131	260 - 545
Vorotetskoe	19	89	Pine	-	518 ± 194	260 - 545
Vorotetskoe	20	99	Pine	-	529 ± 190	260 - 545
Tulgovichskoe	21	110	Birch	54 ± 12	125 ± 44	60 - 112
Tulgovichskoe	22	152	Pine	48 ± 11	96 ± 29	60 - 112
Tulgovichskoe	23	152	Pine	48 ± 11	94 ± 29	60 - 112
Tulgovichskoe	24	213	Pine	67 ± 16	70 ± 19	60 - 112
Tulgovichskoe	25	211	Oak	-	87 ± 23	60 - 112
Tulgovichskoe	26	185	Pine	-	65 ± 18	60 - 112
Tulgovichskoe	27	169	Pine	-	76 ± 23	60 - 112

Matched data are displayed in bold

366

3.6. Future directions

367

368

369

It is clear from the findings of this study that being able to rapidly measure activity activity concentrations of ¹³⁷Cs across the site and in wood using non-destructive *in situ* gamma-ray spectrometry represents a considerable step forward in characterising contaminated forests such

as those found in the Polessie State Radioecology Reserve. The methods capability could certainly become a useful prospecting tool for the forestry industry that could improve decision making as to whether a tree should be felled or not depending on specified regulatory limits. Such an approach might conceivably comprise two phases: (i) in situ or mobile mapping the understory soil contamination levels to highlight likely areas for felling followed by (ii) measurements of tree activity for verification through in situ measurements coupled with a subset of trees being subject to laboratory measurement validation.

The outstanding uncertainties identified by this study were found to be the radial distribution of the contaminant within trees of different species and wood density, which were modelled from preliminary field and literature observations. Understanding how these environmental parameters drive the observed count rate of the system is the next crucial step. For example, accurate characterisation of green wood density is necessary for each individual measurement, although this could be feasibly determined in field using tree cores or modelled using historical data.

Perhaps a more demanding challenge is to reliably account for changes in radial distribution. To accomplish this, large amounts of empirical data will have to be acquired to investigate patterns in the shape of the radial distribution for a given species considering the age and diameter of the tree and perhaps the underlying soil distribution. Current estimates from the models developed in this study suggest that without confident resolution of this parameter final wood activity estimates could be orders of magnitude from the true value and no better than estimates of transfer factors, albeit without the need for physical sampling. Although discrepancies between *in situ* and coring estimates were not found to be to this level within this study, differences at the low activity site could in part be explained by this occurrence.

A final argument for the further development of this *in situ* method is the unpredictability of the core data taken during this study. The results suggest that *in situ* results could in fact be more representative of the true activity value, by showing less statistical variation, than the core values that were used to validate due to the consistency in results displayed across each site.

It must be noted, ^{137}Cs poses less risk to human health compared with ^{90}Sr with regards to wood contamination as strontium is absorbed more readily by trees. However, ^{90}Sr is more difficult to measure in situ as it does not have a significant gamma-ray emission, therefore is only feasible to measure through laboratory equipment.

4. Conclusions

A non-destructive in situ gamma spectrometric method to measure ^{137}Cs contamination in trees has been described and demonstrated in a forest in the Belarusian Chernobyl exclusion zone. The real-time method showed promising agreement with wood activity estimates made using a traditional tree coring device and laboratory gamma-ray spectrometry. Potentially, the method could be widely adopted, alongside mobile gamma-ray spectrometry, negating the need for a tree to be felled and prolonged laboratory measurement of sampled environmental media. Wider investigations into the uncertainties distributions associated with wood density and radial distribution are required. Larger scale datasets are required to parameterise the underlying models used to separate the signal from the tree and the background and the final radial distribution calibration factor to derive wood activity.

Acknowledgements

The authors are grateful to the workers of the scientific part of the Polessie State Radiation Ecology Reserve: V. Kalinin, E. Kalyhan, N. Dzemenkavets, A. Masheuski, N. Blinova, A. Uhlianets and D. Garbaruk for fieldwork, sample preparation and laboratory analysis.

5. References

- Auty, D., Achim, A., Macdonald, E., Cameron, A.D., Gardiner, B.A., 2014. Models for predicting wood density variation in Scots pine. *Forestry* 87, 449–458. <https://doi.org/10.1093/forestry/cpu005>
- Beck, H., DeCampo, J., Gogolak, C., 1972. In situ Ge(Li) and NaI(Tl) gamma-ray spectrometry. New York. <https://doi.org/10.2172/4599415>
- Benke, R.R., Kearfott, K.J., 2002. Demonstration of a collimated in situ method for determining depth distributions using g-ray spectrometry, *Nuclear Instruments and Methods in Physics Research A*.
- Briesmeister, J.F., 1993. MCNP-A general Monte Carlo N-particle transport code. LA-12625.
- Cresswell, A.J., Kato, H., Onda, Y., Nanba, K., 2016. Evaluation of forest decontamination using radiometric measurements. *J. Environ. Radioact.* 164, 133–144. <https://doi.org/10.1016/j.jenvrad.2016.07.024>
- de Groot, A. V., van der Graaf, E.R., de Meijer, R.J., Maučec, M., 2009. Sensitivity of in-situ γ -ray spectra to soil density and water content. *Nucl. Instruments Methods Phys. Res. Sect. A Accel. Spectrometers, Detect. Assoc. Equip.* 600, 519–523. <https://doi.org/10.1016/j.nima.2008.12.003>
- Dvornik, A.A., Dvornik, A.M., Korol, R.A., Shamal, N. V., Gaponenko, S.O., Bardyukova, A. V., 2018. Potential threat to human health during forest fires in the Belarusian exclusion zone. *Aerosol Sci. Technol.* 52, 923–932. <https://doi.org/10.1080/02786826.2018.1482408>
- Evangeliou, N., 2015. Fire evolution in the radioactive forests of Ukraine and Belarus: future risks for the population and the environment. *Ecol. Monogr.* 85, 49–72.
- Feng, T.C., Jia, M.Y., Feng, Y.J., 2012. Method-sensitivity of in-situ gamma spectrometry to determine the depth-distribution of anthropogenic radionuclides in soil. *Nucl. Instruments Methods Phys. Res. Sect. A-Accelerators Spectrometers Detect. Assoc. Equip.* 661, 26–30. <https://doi.org/10.1016/j.nima.2011.09.014>

449 Fogh, C.L., Andersson, K.G., 2001. Dynamic behaviour of ^{137}Cs contamination in trees of the
 450 Briansk region, Russia. *Sci. Total Environ.* 269, 105–115. [https://doi.org/10.1016/S0048-](https://doi.org/10.1016/S0048-9697(00)00819-6)
 451 9697(00)00819-6

452 Gerasimov, Y., Karjalainen, Y., 2010. (PDF) Atlas of the forest sector in Belarus. Work. Pap.
 453 Finnish For. Res. Inst. 170Publisher Finnish For.

454 Gering, C.F., Kiefer, P., Fesenko, S., Voigt, G., 2002. In situ gamma-ray spectrometry in
 455 forests: determination of kerma rate in air from. *J. Environ. Radioact.* 61, 75–89.

456 Golosov, V., 2003. Application of Chernobyl-derived ^{137}Cs for the assessment of soil
 457 redistribution within a cultivated field. *Soil Tillage Res.* [https://doi.org/10.1016/S0167-](https://doi.org/10.1016/S0167-1987(02)00130-7)
 458 1987(02)00130-7

459 Golosov, V.N.V., Walling, D., Kvasnikova, E.V.E., Stukin, E.D., Nikolaev, A.N., Panin, A. V.,
 460 2000. Application of a field-portable scintillation detector for studying the distribution of
 461 ^{137}Cs inventories in a small basin in Central Russia. *J. Environ. Radioact.* 48, 79–94.
 462 [https://doi.org/10.1016/S0265-931X\(99\)00058-2](https://doi.org/10.1016/S0265-931X(99)00058-2)

463 Goor, F., Avila, R., 2003. Quantitative comparison of models of ^{137}Cs cycling in forest
 464 ecosystems. *Environ. Model. Softw.* 18, 273–279. [https://doi.org/10.1016/S1364-](https://doi.org/10.1016/S1364-8152(02)00075-0)
 465 8152(02)00075-0

466 Goor, F., Davydchuk, V., Vandenhove, H., 2003. GIS-based methodology for Chernobyl
 467 contaminated land management through biomass conversion into energy - A case study
 468 for Polessie, Ukraine. *Biomass and Bioenergy* 25, 409–421.
 469 [https://doi.org/10.1016/S0961-9534\(03\)00034-5](https://doi.org/10.1016/S0961-9534(03)00034-5)

470 Goor, F., Thiry, Y., 2004. Processes, dynamics and modelling of radiocaesium cycling in a
 471 chronosequence of Chernobyl-contaminated Scots pine (*Pinus sylvestris* L.) plantations.
 472 *Sci. Total Environ.* 325, 163–180. <https://doi.org/10.1016/j.scitotenv.2003.10.037>

473 Harrison, R.L., 2009. Introduction to Monte Carlo simulation, in: *AIP Conference Proceedings*.
 474 pp. 17–21. <https://doi.org/10.1063/1.3295638>

475 IAEA, 2008. Environmental consequences of the Chernobyl accident and their remediation: 20
 476 years of experience. *Chernobyl.* <https://doi.org/10.1093/rpd/ncl163>

477 Ipatyev, V., Bulavik, I., Baginsky, V., Goncharenko, G., Dvornik, A., 1999. Forest and
 478 Chernobyl: Forest ecosystems after the Chernobyl nuclear power plant accident: 1986-
 479 1994. *J. Environ. Radioact.* 42, 9–38. [https://doi.org/10.1016/S0265-931X\(98\)00042-3](https://doi.org/10.1016/S0265-931X(98)00042-3)

480 Izrael, Y.A., De Cort, M., Jones, A.R., Nazarov, I.M., Fridman, S.D., Kvasnikova, E. V., Stukin,
 481 E.D., Kelly, G.N., Matveenکو, I.I., Pokumeiko, Y.M., Tabatchnyi, L.Y., Tsaturon, Y.,
 482 1996. The atlas of caesium-137 contamination of Europe after the Chernobyl accident.
 483 *Radiol. consequences Chernobyl Accid.* 1–10.

484 Kirk, B.L., 2010. Overview of Monte Carlo radiation transport codes, in: *Radiation*
 485 *Measurements*. Pergamon, pp. 1318–1322. <https://doi.org/10.1016/j.radmeas.2010.05.037>

486 Likar, A., Vidmar, T., Lipoglavsek, M., Omahen, G., 2004. Monte Carlo calculation of entire
 487 in situ gamma-ray spectra. *J. Environ. Radioact.* 72, 163–168.

488 Malins, A., Okumura, M., Machida, M., Takemiya, H., Saito, K., 2015. Fields of View for
 489 *Environmental Radioactivity* 2–7.

490 Maučec, M., De Meijer, R.J., Van Der Klis, M.M.I.P., Hendriks, P.H.G.M., Jones, D.G., 2004.
 491 Detection of radioactive particles offshore by gamma-ray spectrometry Part II: Monte
 492 Carlo assessment of acquisition times. *Nucl. Instruments Methods Phys. Res. Sect. A*
 493 *Accel. Spectrometers, Detect. Assoc. Equip.* 525, 610–622.
 494 <https://doi.org/10.1016/j.nima.2004.01.075>

495 Maučec, M., Hendriks, P.H.G.M., Limburg, J., de Meijer, R.J., 2009. Determination of
 496 correction factors for borehole natural gamma-ray measurements by Monte Carlo
 497 simulations. *Nucl. Instruments Methods Phys. Res. Sect. A Accel. Spectrometers, Detect.*
 498 *Assoc. Equip.* 609, 194–204. <https://doi.org/http://dx.doi.org/10.1016/j.nima.2009.08.054>

499 Melin, J., Wallberg, L., Suomela, J., 1994. Distribution and retention of cesium and strontium
 500 in Swedish boreal forest ecosystems. *Sci. Total Environ.* 157, 93–105.
 501 [https://doi.org/10.1016/0048-9697\(94\)90568-1](https://doi.org/10.1016/0048-9697(94)90568-1)

502 Miller, K.M., Kuiper, J.L., Helfer, I.K., 1990. ¹³⁷Cs fallout depth distributions in forest versus
 503 field sites: Implications for external gamma dose rates. *J. Environ. Radioact.* 12, 23–47.
 504 [https://doi.org/10.1016/0265-931X\(90\)90034-S](https://doi.org/10.1016/0265-931X(90)90034-S)

505 Myttenaere, C., Schell, W.R., Thiry, Y., Sombre, L., Ronneau, C., van der Stegen de Schrieck,
506 J., 1993. Modelling of Cs-137 cycling in forests: recent developments and research needed.
507 Sci. Total Environ. 136, 77–91. [https://doi.org/http://dx.doi.org/10.1016/0048-](https://doi.org/http://dx.doi.org/10.1016/0048-9697(93)90298-K)
508 9697(93)90298-K

509 Narayan, R.D., Miranda, R., Rez, P., 2012. Monte Carlo simulation for the electron cascade
510 due to gamma rays in semiconductor radiation detectors. J. Appl. Phys. 111, 64910.
511 <https://doi.org/10.1063/1.3698370>

512 Nimis, P.L., 1996. RADIOCESIUM IN PLANTS OF FOREST ECOSYSTEMS, Studia
513 Geobotanica.

514 Ohashi, S., Okada, N., Tanaka, A., Nakai, W., Takano, S., 2014. Radial and vertical
515 distributions of radiocesium in tree stems of *Pinus densiflora* and *Quercus serrata* 1.5 y
516 after the Fukushima nuclear disaster. J. Environ. Radioact. 134, 54–60.
517 <https://doi.org/10.1016/j.jenvrad.2014.03.001>

518 Östlund, K., Samuelsson, C., Rääf, C.L., 2015. Experimentally determined vs: Monte Carlo
519 simulated peak-to-valley ratios for a well-characterised n-type HPGe detector. Appl.
520 Radiat. Isot. <https://doi.org/10.1016/j.apradiso.2014.09.022>

521 RDU/LH-2001, 2001. Republican permissible levels of content of ¹³⁷Cs in wood, products
522 from wood and wood materials and other non-edible products of forestry (in Russian).

523 Shaw, G., Robinson, C., Holm, E., Frissel, M.J., Crick, M., 2001. A cost-benefit analysis of
524 long-term management options for forests following contamination with ¹³⁷Cs. J.
525 Environ. Radioact. 56, 185–208. [https://doi.org/10.1016/S0265-931X\(01\)00053-4](https://doi.org/10.1016/S0265-931X(01)00053-4)

526 Sheppard, S.C., 2005. Transfer parameters-Are on-site data really better? Hum. Ecol. Risk
527 Assess. <https://doi.org/10.1080/10807030500257747>

528 Soukhova, N. V, Fesenko, S. V, Klein, D., Spiridonov, S.I., Sanzharova, N.I., Badot, P.M.,
529 2003. Cs distribution among annual rings of different tree species contaminated after the
530 Chernobyl accident, Journal of Environmental Radioactivity.

531 Strandgard, M., Walsh, D., 2011. Improving harvester estimates of bark thickness for radiata
532 pine (*Pinus radiata* D.Don). South. For. a J. For. Sci. 73, 101–108.

533 <https://doi.org/10.2989/20702620.2011.610876>

534 Thiessen, K.M., Thorne, M.C., Maul, P.R., Pröhl, G., Wheeler, H.S., 1999. Modelling
 535 radionuclide distribution and transport in the environment, in: Environmental Pollution.
 536 Elsevier Science Ltd, pp. 151–177. [https://doi.org/10.1016/S0269-7491\(99\)00090-1](https://doi.org/10.1016/S0269-7491(99)00090-1)

537 Thiry, Y., Garcia-Sanchez, L., Hurtevent, P., 2015. Experimental quantification of radiocesium
 538 recycling in a coniferous tree after aerial contamination: Field loss dynamics, translocation
 539 and final partitioning. J. Environ. Radioact. 161, 42–50.
 540 <https://doi.org/10.1016/j.jenvrad.2015.12.017>

541 Thiry, Y., Goor, F., Riesen, T., 2002. The true distribution and accumulation of radiocaesium
 542 in stem of Scots pine (*Pinus sylvestris* L.). J. Environ. Radioact. 58, 243–259.
 543 [https://doi.org/10.1016/S0265-931X\(01\)00068-6](https://doi.org/10.1016/S0265-931X(01)00068-6)

544 Tyler, A.N., 2008. In situ and airborne gamma-ray spectrometry, in: Radioactivity in the
 545 Environment, Analysis of Environmental Radionuclides. Elsevier, pp. 407–448.
 546 [https://doi.org/10.1016/S1569-4860\(07\)11013-5](https://doi.org/10.1016/S1569-4860(07)11013-5)

547 van der Perk, M., Burema, J., Vandenhove, H., Goor, F., Timofeyev, S., 2004. Spatial
 548 assessment of the economic feasibility of short rotation coppice on radioactively
 549 contaminated land in Belarus, Ukraine, and Russia. I. model description and scenario
 550 analysis. J. Environ. Manage. 72, 217–232.
 551 <https://doi.org/10.1016/j.jenvman.2004.05.002>

552 Varley, A., Tyler, A., Bondar, Y., Hosseini, A., Zabrotski, V., Dowdall, M., 2018.
 553 Reconstructing the deposition environment and long-term fate of Chernobyl ¹³⁷Cs at the
 554 floodplain scale through mobile gamma spectrometry. Environ. Pollut. 240, 191–199.
 555 <https://doi.org/10.1016/J.ENVPOL.2018.04.112>

556 Varley, Adam, Tyler, A., Dowdall, M., Bondar, Y., Zabrotski, V., 2017. An in situ method for
 557 the high resolution mapping of ¹³⁷Cs and estimation of vertical depth penetration in a
 558 highly contaminated environment. Sci. Total Environ. 605–606, 957–966.
 559 <https://doi.org/10.1016/j.scitotenv.2017.06.067>

560 Varley, A., Tyler, A., Dowdall, M., Bondar, Y., Zabrotski, V., 2017. An in situ method for the

high resolution mapping of¹³⁷Cs and estimation of vertical depth penetration in a highly
contaminated environment. Sci. Total Environ. 605–606.
<https://doi.org/10.1016/j.scitotenv.2017.06.067>

Vitaly, L., Sokolov, A., Saveliev, A.A., 2019. Spatial analysis and modeling of cesium-137
redistribution in the soil cover of the Bryansk region Spatial analysis and modeling of
cesium-137 redistribution in the soil cover of the Bryansk region, in: EGU General
Assembly 2019At: Viena, Austria.

Vitaly, L., Sokolov, A., Saveliev, A.A., Mironenko, I. V, 2018. Landscape-scale modelling to
predict soil lateral migration using Cs-137 on the Bryansk Opolje region (Russia) In :
GlobalSoilMap Digital Soil Mapping from Country to Globe Eds . Dom ..., in:
GlobalSoilMap.

Woodfuels Program, E., 2009. Program to set up the production of wood pellets (pellets), wood
briquettes and coal in the organizations of the Ministry of Forestry 2009-2011 (in Russian).

Yoshihara, T., Matsumura, H., Tsuzaki, M., Wakamatsu, T., Kobayashi, T., Hashida, S. nosuke,
Nagaoka, T., Goto, F., 2014. Changes in radiocesium contamination from fukushima in
foliar parts of 10 common tree species in Japan between 2011 and 2013. J. Environ.
Radioact. 138, 220–226. <https://doi.org/10.1016/j.jenvrad.2014.09.002>